Geomechanics and Engineering, *Vol. 30, No. 4 (2022) 383-392*
https://doi.org/10.12989/gae.2022.30.4.383

Three-dimensional numerical parametric study of tunneling effects on existing pipelines

Jiangwei Shi[1], Jinpu Wang[1], Xiaojia Ji[2], Huaqiang Liu[3] and Hu Lu*[4]

[1]*Key Laboratory of Ministry of Education for Geomechanics and Embankment Engineering, Hohai University, Nanjing, Jiangsu 210024, China*
[2]*Intelligent Safe Collaborative Innovation Center, Zhejiang College of Security Technology, Wenzhou 325016, China*
[3]*Material and Structural Engineering Department of Jiangsu Water Research Institute, Yangzhou 225000, China*
[4]*Shenzhen Polytechnic, No. 7098 Liu Xian Avenue, Nanshan District, Shenzhen, China*

(*Received June 13, 2022, Revised July 22, 2022, Accepted July 29, 2022*)

Abstract. Although pipelines are composed of segmental tubes commonly connected by rubber gasket or push-in joints, current studies mainly simplified pipelines as continuous structures. Effects of joints on three-dimensional deformation mechanisms of existing pipelines due to tunnel excavation are not fully understood. By conducting three-dimensional numerical analyses, effects of pipeline burial depth, tunnel burial depth, volume loss, pipeline stiffness and joint stiffness on bending strain and joint rotation of existing pipelines are explored. By increasing pipeline burial depth or decreasing tunnel cover depth, tunneling-induced pipeline deformations are substantially increased. As tunnel volume loss varies from 0.5% to 3%, the maximum bending strains and joint rotation angles of discontinuous pipelines increase by 1.08 and 9.20 times, respectively. By increasing flexural stiffness of pipe segment, a dramatic increase in the maximum joint rotation angles is observed in discontinuous pipelines. Thus, the safety of existing discontinuous pipelines due to tunnel excavation is controlled by joint rotation rather than bending strain. By increasing joint stiffness ratio from 0.0 (i.e., completely flexible joints) to 1.0 (i.e., continuous pipelines), tunneling-induced maximum pipeline settlements decrease by 22.8%-34.7%. If a jointed pipeline is simplified as a continuous structure, tunneling-induced settlement is thus underestimated, but bending strain is grossly overestimated. Thus, joints should be directly simulated in the analysis of tunnel-soil-pipeline interaction.

Keywords: bending strain; joint rotation; pipeline; three-dimensional; tunnel

1. Introduction

In congested urban cities, it is not uncommon to construct new tunnels below existing underground pipelines. Because of tunnel excavation, stress changes are induced in the ground, leading additional stress changes and differential deformations to existing pipelines (Shi *et al*. 2017, Rebello *et al*. 2018, Fang *et al*. 2022). To ensure the serviceability and safety of existing pipelines due to tunnel excavation, many studies have been conducted to investigate the complex tunnel-soil-pipeline interaction.

By using Winkler-based and elastic continuum models, a series of analytical solutions (Attewell *et al*. 1986, Vorster *et al*. 2005, Klar *et al*. 2005, Franza and Marshall 2019) were proposed to calculate bending strains of existing continuous pipelines due to tunnel excavation. Moreover, Ieronymaki *et al*. (2017) proposed a method for estimating bending moment and axial load of continuous pipelines. In those studies, soil was assumed as an elastic material with a constant modulus. To evaluate effects of burial depth on pipeline responses due to tunnel excavation, Yu *et al*. (2013) proposed an expression for Winkler subgrade modulus of a pipeline buried at any depths. By using Pasternak beam theory, Zhu *et al*. (2020) found that shear stiffness of pipeline had little effects on pipeline settlements. By applying free field displacements as boundary conditions, Zhang *et al*. (2021) proposed a simplified analytical solution for calculating deformations of continuous pipelines due to quasi-rectangular tunnel excavation. However, all those studies simplified existing pipelines as continuous structures, and only focused on bending behavior of existing pipelines.

If pipe segments were connected by rubber gasket or push-in joints, they were typical discontinuous structures. Both bending moment and joint rotation were expected to be induced in existing pipeline due to tunneling. Water or oil leakage may occur if tunneling-induced joint rotation exceeds a certain allowable value (Molnar *et al*. 2003). As far as the authors are aware, studies on the responses of jointed pipeline due to tunnel excavation were limited. By using an elastic continuum method, Klar *et al*. (2008) proposed an analytical solution for estimating tunneling induced joint rotation angle in discontinuous pipeline. Based on the Winkler model, Huang *et al*. (2019) proposed an improved Winkler modulus to analyze responses of jointed pipelines due to underneath tunnel excavation. By conducting a two-dimensional numerical parametric study, Shi *et al*. (2016a) proposed calculation charts for direct estimation of joint rotation angles of discontinuous pipelines due to tunnel excavation. Based on two-dimensional numerical modelling, Wham *et al*. (2016) investigated responses of jointed cast iron and ductile

*Corresponding author, Lecturer
E-mail: lvhu1212@163.com

ISSN: 2005-307X (Print), 2092-6219 (Online)

pipelines due to underneath tunnel excavation. It was found that ductile iron pipelines had much more ability to against joint leakage than cast iron pipelines. However, those studies simplified the tunnel-soil-pipeline interaction as a plane strain problem, ignoring three-dimensional deformations of existing pipelines due to tunnel excavation (Shi *et al*. 2016b). By conducting three-dimensional centrifuge tests, several studies investigated the influence on joint stiffness on pipeline response (Huang *et al*. 2014, Saiyar *et al*. 2015, Shi *et al*. 2022a). In those studies, tubes with small stiffness were used to connect to pipe segments. In other words, pipeline joints were simulated by a weak material.

By conducting three-dimensional centrifuge tests, Ma *et al*. (2018) explored the influence of construction sequences of double-stacked tunnels on existing pipelines. It was found that much larger settlement and bending strain were induced in the existing pipeline when the upper tunnel was excavated first. Based on three-dimensional centrifuge test results, Shi *et al*. (2016b) found that tunneling-induced major influence zone of pipe settlement and strain was located within ±1.25 *D* (i.e., tunnel diameter). It was well-known that soil stiffness was stress, strain and stress path dependent (Clayton 2011). As tunnel excavation proceeded further, stiffness of soil surrounding existing pipeline is expected to be decreased. However, linear elastic and perfectly plastic models such as Mohr-Coulomb failure criteria were widely used to analyze responses of existing pipelines due to tunnel excavation (e.g., Zhang *et al*. 2016, Zhang *et al*. 2019, Guan *et al*. 2020). Without considering small strain soil stiffness, the computed ground settlement trough induced by tunnel excavation was normally wide and shallow (Addenbrooke *et al*. 1997). To obtain a reasonable estimation of tunneling-induced pipeline responses, small strain soil stiffness should be directly considered by an advanced constitutive soil model (e.g., Ardakani *et al*. 2014, Ma *et al*. 2017, Wang *et al*. 2018).

In this paper, three-dimensional numerical analyses were conducted to investigate deformation characteristics of continuous and jointed pipelines due to underneath tunnel excavation. A hardening soil model with consideration of small strain soil stiffness (HSS) was adopted to capture stress and strain level dependent soil behaviors. The validity of soil model and soil parameters was verified by three-dimensional centrifuge test results. By conducting an extensive numerical parametric study, effects of pipeline burial depth, tunnel burial depth, volume loss, joint stiffness and pipeline stiffness on bending strain and joint rotation of existing pipelines were explored. By comparing computed results of continuous and jointed pipelines, effects of joint stiffness on pipeline deformations were analyzed.

2. Three-dimensional numerical back-analysis of centrifuge test

2.1 Three-dimensional centrifuge test

Before conducting any numerical parametric study, centrifuge test results were adopted to calibrate soil model and model parameters. As reported by Shi *et al*. (2016b), a new tunnel was constructed crossing an existing pipeline in dry Toyoura sand. In this test, the length, width and height of soil sample were 1245, 990 and 700 mm, corresponding to 49.8, 39.6 and 28 m in prototype, respectively. The mode pipeline was made of aluminum alloy tube with a length (L_p), a diameter (d_p) and a wall thickness (w_p) of 920 mm, 15.88 mm and 1.65 mm, which were equivalent to 36.8, 0.635, and 0.066 m, respectively. The diameter of model tunnel (D) was 152 mm, corresponding to 6.08 m in prototype, which was a common diameter of shield tunnel in practice. The burial depths of the model pipeline (c_p) and the model tunnel (C) were 30 mm and 225 mm, corresponding to 1.2 m and 9.0 m, respectively. Thus, the tunnel cover depth to diameter ratio (C/D) was 1.48, which was also a typical value in practice. The model tunnel consisted of seven pairs of cylindrical rubber bags, which were filled with de-aired water. Excavation length of each excavation segment was 76 mm, which was 0.5 times of tunnel diameter. A well-controlled amount of water (i.e., 2% of tunnel volume loss) was drained away in seven steps. The averaged dry density (ρ_d) of Toyoura sand was 1550 kg/m³, corresponding to a relative sand density (D_r) of 68%. Details of this centrifuge test were given in Shi *et al*. (2016b).

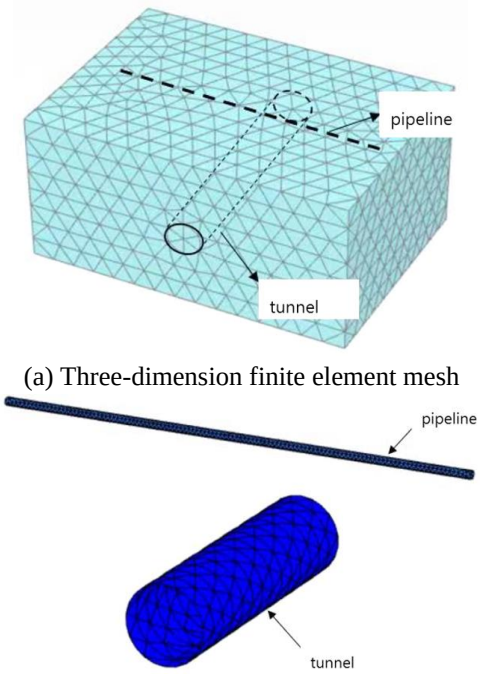

(a) Three-dimension finite element mesh

(b) Model tunnel and model pipeline

Fig. 1 Three-dimension numerical mesh of tunnel-pipeline interaction

2.2 Numerical model for back-analyzing centrifuge test

Fig. 1 shows the three-dimensional finite element mesh used to back-analyze the centrifuge test. Shell elements were used to simulate the model pipeline and tunnel lining, while 10 noded tetrahedron elements were used to model soil stratum. This three-dimensional mesh consisted of

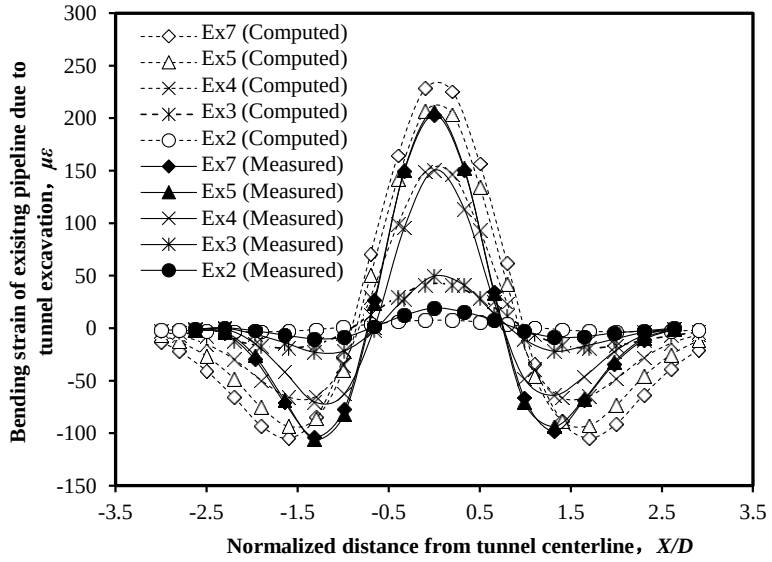

Fig. 2 Comparison of the measured and computed bending strains of pipeline due to tunnel excavation

Table 1 Parameters of HHS model for Toyoura sand

Parameters	Value
Secant modulus, E_{50}^{ref} (MPa)	35.0
Tangent oedometric modulus, E_{oed}^{ref} (MPa)	35.0
Unloading-reloading modulus, E_{ur}^{ref} (MPa)	105.0
Modulus stress related power exponent, m	0.8
Effective cohesion, c' (kPa)	1.0
Effective friction angle, φ' (°)	31.0
Reference shear modulus, $\gamma_{0.7}$	3.5×10^{-4}
Reference initial shear modulus, G_0^{ref} (MPa)	280.0
Coefficient of lateral pressure K_0	0.49
Failure ratio R_f	0.90

29094 elements and 37694 nodes. By increasing the numbers of elements and nodes to 49218 and 65378, the maximum settlement of pipeline was only differed by 1.1%. It was indicated that the current mesh density was already fine enough. Soil movements perpendicular to the four vertical faces of the mesh were constrained, while soil movements at the bottom of the mesh were constrained in three directions.

In this study, the excavation length of tunnel was 3.5 times of the tunnel diameter. Based on the centrifuge test results, tunnelling-induced pipeline responses were negligible when the tunnel face was ±1.25 D away from the pipeline centerline (Shi *et al*. 2016b). Moreover, the bending stains induced at the two ends of pipeline were close to zero. It was indicated that the lengths of tunnel excavation and pipeline were long enough to eliminate boundary effects.

The existing pipelines were assumed to be wished-in-place. In other words, the effects of pipeline installation effects were not considered. To back-analysis the centrifuge model test, numerical modelling procedures were the same as that of the centrifuge test. Firstly, the initial ground conditions were established by applying a K_0 value of 0.491. For each excavation step, tunnel excavation was of soil within tunnel. Along the circumferential direction of tunnel lining, the surface was contracted by 2% to simulate tunneling-induced volume loss.

2.3 Constitutive model and model parameters

As reported in literature, shear strains of soil surrounding existing tunnel and diaphragm wall were in a typical range of 0.01% to 0.1% (i.e., Clayton 2011, Shi *et al*. 2022b). For soil strain within small strain level, soil stiffness was greatly degraded as an increase in soil strain. Obviously, the accuracy of computed ground and pipeline response due to tunnel excavation depended on the reasonable simulation of small-strain soil stiffness. In this study, hardening soil model with small-strain stiffness (HSS) was used to simulate soil responses, while an elastic model was used to simulate pipeline responses. By conducting triaxial tests, the internal shearing frictional angle and cohesion were 31° and 1 kPa, respectively. By using the small strain stiffness curve reported by Yamashita *et al*. (2000), the soil parameters of HSS model were calibrated. A summary of soil parameters of HHS model was given in Table 1.

2.3 Comparisons of the measured and computed strains induced in the pipeline along its longitudinal direction

Fig. 2 compares the measured and computed bending strains of pipeline along its longitudinal direction due to underlying tunnel excavation. The positive and negative values denote tensile and compressive strains at the pipeline invert level, respectively. The legend "Ex2-7" denotes tunnel excavation stages. Due to tunnel excavation-induced differential pipeline settlements, sagging moments (i.e., tensile strains) are induced in the pipeline above tunnel center line, while hogging moments (i.e., compressive strains) are induced in the pipeline at the two sides of the model tunnel. As expected, bending strain of pipeline

Table 2 Summary of numerical analyses of tunnel-soil-pipeline interaction

Series	Burial depth ratio (c_p/C_T)	Joint stiffness ratio (R_j/R_p)	Tunnel cover depth to diameter ratio (C/D)	Pipeline stiffness, EI (MN·m^2)	Volume loss (VL)
C_p	0.2, 0.4, 0.6, 0.8	0.0, 1.0	2.0	3.39×10^2	2%
C	0.2	0.0, 1.0	1.0, 1.5, 2.0, 2.5, 3.0	3.39×10^2	2%
VL	0.2	0.0, 1.0	2.0	3.39×10^2 6.30×10^3	0.5%, 1%, 1.5%, 2%, 2.5%, 3%
R_j	0.2	0.0, 0.1, 0.25, 0.5, 0.75, 1.0	2.0	3.39×10^2 6.30×10^3	2%

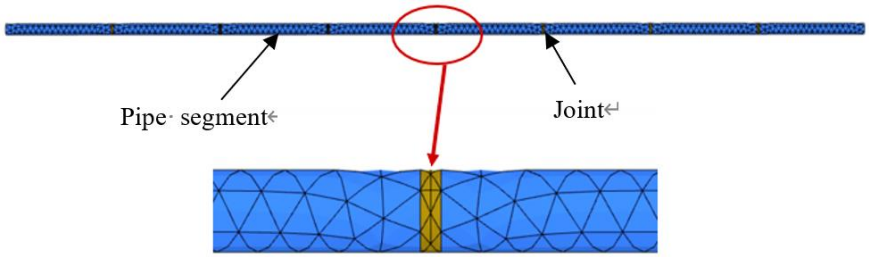

Fig. 3 An illustration of jointed pipeline in the numerical simulation

increases as tunnel proceeds further. Upon completion of the tunnel excavation, the computed and measured maximum tensile strains are 234.6 and 206.3 με, respectively. Moreover, the computed and measured maximum compressive strains are 104.7 and 93.7 με, respectively. The computed maximum tensile and compressive strains are about 12-14% larger than that the measured values. It is indicated that the numerical modelling procedures and model parameters are reasonable. Since the computed pipeline strains are slightly larger than the measured values, numerical analysis conducted in this study can provide a conservative estimation of pipeline response due to tunnel excavation.

3. Three-dimensional numerical parametric study

3.1 Numerical analysis program

In this study, effects of pipeline burial depth, tunnel cover depth, volume loss, joint stiffness and pipeline stiffness on pipeline responses due to tunnel excavation were explored. The ratio of pipeline burial depth (c_p) to the tunnel cover depth (C) varied from 0.1-0.8 (1.2-9.6 m). The cover depth to tunnel diameter ratio (C/D) was 1.0, 1.5, 2.0, 2.5 and 3.0. The cover depths of existing pipeline and tunnel are common values used in practice (e.g., Tan and Wei 2011, Ng *et al*. 2013, Lu *et al*. 2020, Soomro *et al*. 2020). Based on previous studies, construction of tunnel using earth pressure balance machine in sand and clay caused a volume loss in a range of 1%-4% (Shirlaw *et al*. 2003). To evaluate the effects of volume loss on pipeline responses, a relatively large range of volume loss was designed as 0.5% to 3%. For jointed pipeline, ratio of joint stiffness (R_j) to pipe segment stiffness (R_p) varied from 0.0 (i.e., completely flexible joint) to 1.0 (i.e., continuous pipeline). To assess the influence of pipeline stiffness on bending strain and joint rotation, two typical pipelines, namely flexible and stiff pipelines were designed. The flexural stiffnesses of the flexible and stiff pipelines were 3.39×10^2 MN·m^2 and 6.30×10^3 MN·m^2, respectively. The flexible pipeline (i.e., FP) had an equivalent flexural stiffness of concrete pipelines with an outer diameter of 800 mm and a wall thickness of 65 mm. A concrete pipe with an outer diameter of 1680 mm and a wall thickness of 120 mm had the same flexural stiffness of the stiff pipeline (i.e., SP) adopted in this study. In total, 48 numerical analyses were conducted to investigated three-dimensional responses of continuous and jointed pipelines due to tunnel excavation, as summarized in Table 2.

3.2 Simulation of pipeline joints

Compared with continuous pipelines, joints were weak points of discontinuous pipelines. In reality, the length of pipe segments and joints commonly varied from 4 to 8 m and 0.1 to 0.2 m, respectively. In practice, deformation behaviors were really complicated at the pipeline joints. In the numerical analysis, a simplified method was used to simulate jointed pipelines. The weakness of the joint was simulated by applying a reduction factor to Young's modulus. By reducing the Young's modulus of the joint, the influence of different joint stiffness on pipeline deformation was explored. Since method had the ability to capture the key deformation behavior of pipeline joints, it was extensively used in the previous studies (Huang *et al*. 2014, Saiyar *et al*. 2015, Shi *et al*. 2022a).

In this study, the jointed pipeline consisted of eight pipe segments and seven joints, as shown in Fig. 3. The lengths of pipe segment and joint were 6 m and 0.16 m, respectively, which were typical values in practice (Klar *et al*. 2008). Because of tunnel excavation, differential settlements were induced in the existing pipelines. Based on the numerical results, settlements at the joint and pile segment closest to the joint can be obtained. Joint rotation was calculated by differential settlements between joint and pipe segment divided by horizontal distance between those two monitoring points.

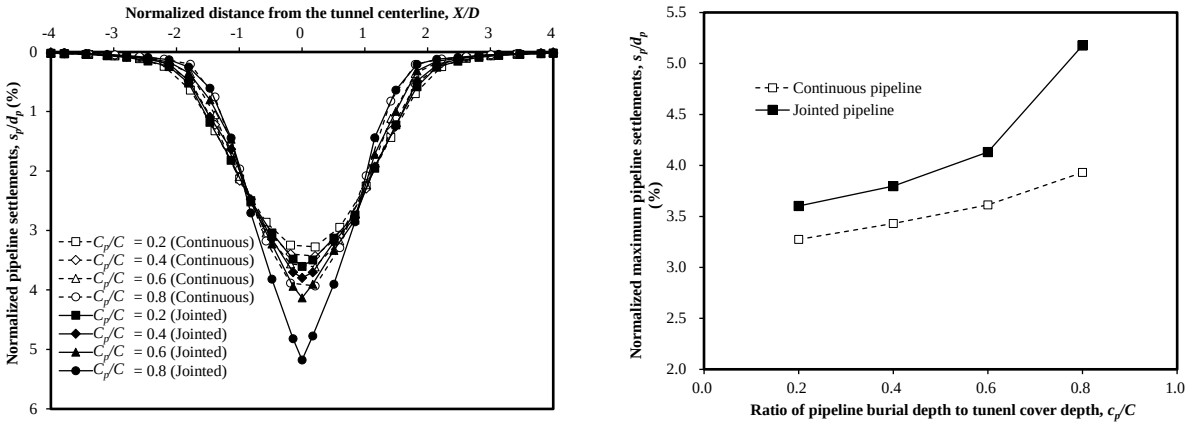

(a) (b)

Fig. 4 Effects of pipe burial depth on tunneling-induced maximum pipeline settlements

4. Interpretation of the computed results

4.1 Effects of pipeline burial depth on pipeline responses

Fig. 4(a) shows variations of tunneling-induced settlements in continuous pipelines with pipeline burial depth. The pipeline settlement (s_p) is normalized by the outer diameter of pipeline (d_p). Parameters C_p, C and D are pipeline burial depth, tunnel burial depth and tunnel diameter, respectively. As expected, the maximum pipeline settlement occurs above the tunnel center line, and pipeline settlement decreases rapidly by increasing the normalized distance from tunnel centerline. When the normalized distance from tunnel centerline reaches 2 times of tunnel diameter, tunneling-induced pipeline settlement is negligible. In other words, tunneling-induced major influence zone of pipeline settlement along the transverse tunnel direction is within ±2 D.

When the burial depths of the existing pipelines are 0.2C, 0.4C, 0.6C and 0.8C (i.e., tunnel cover depth), tunneling-induced maximum settlements in the continuous pipelines are 3.27%d_p, 3.43%d_p, 3.61%d_p and 3.93%d_p, respectively. Obviously, the existing pipeline is located much closer to the new tunnel by increasing the burial depth of the existing pipeline. Accordingly, the existing pipeline suffers much larger stress relief due to tunnel excavation. Thus, tunneling-induced maximum pipeline settlement increases with the pipeline burial depth, at an increased rate.

For tunnel excavated underneath a jointed pipeline, the settlement profile of pipeline is not smooth. It means that rotation angles are induced at the joints. For the pipes buried at depths of 0.2C, 0.4C, 0.6C and 0.8C, tunnel excavation-induced maximum pipeline settlements are 3.60%d_p, 3.80%d_p, 4.13%d_p and 5.18%d_p, respectively. By increasing the burial depth of existing pipelines from 0.2C to 0.8C, tunneling-induced maximum settlements in continuous and jointed pipelines increase by 20.2% and 43.8%, respectively. Obviously, settlements of jointed pipeline are more sensitive to pipeline burial depth. For the burial depth considered in this study, settlements of jointed pipelines are 10.1%-31.8% larger than that of continuous pipelines. This is because joint rotation releases bending constraints along the existing pipeline. Correspondingly, the jointed pipeline has much less resistance to deform with surrounding soils. If a jointed pipeline is simplified a continuous structure without an appropriate reduction of pipeline bending stiffness, tunneling-induced pipeline settlements are thus grossly underestimated.

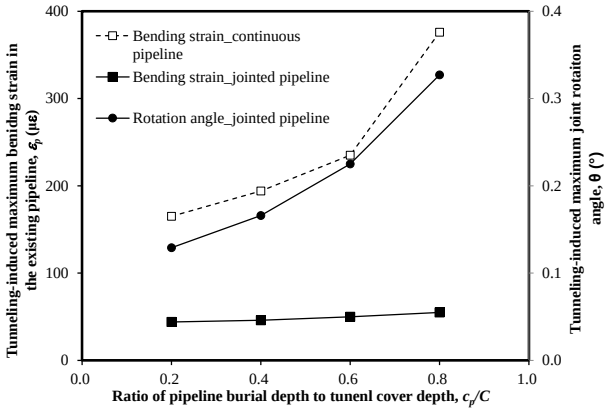

Fig. 5 Effects of pipe burial depth on tunneling-induced bending strains and joint rotation angles

Fig. 5 shows the effects of the pipeline burial depth on tunneling-induced maximum joint rotation angle and maximum bending strain in the existing pipelines. For continuous pipelines, only bending moments are induced by tunnel excavation. In contrast, bending moment and joint rotation are induced simultaneously in the jointed pipelines. When the burial depths of the existing pipelines are 0.2C, 0.4C, 0.6C, and 0.8C, tunneling-induced maximum bending strains in the continuous pipelines are 165, 194, 235 and 376 $\mu\varepsilon$, respectively. As the new tunnel is constructed closer to the existing pipeline, tunneling-induced bending strain is increased at an increased rate. When there are joints in the existing pipelines, tunneling-induced maximum bending strains are substantially reduced. For jointed pipeline buried at depths of 0.2 to 0.8C, tunneling-induced maximum bending strains are in a range of 44 to 55 $\mu\varepsilon$, which are only 14.6%-26.7% of that induced in the continuous pipelines. This is because joint rotation occurred in discontinuous

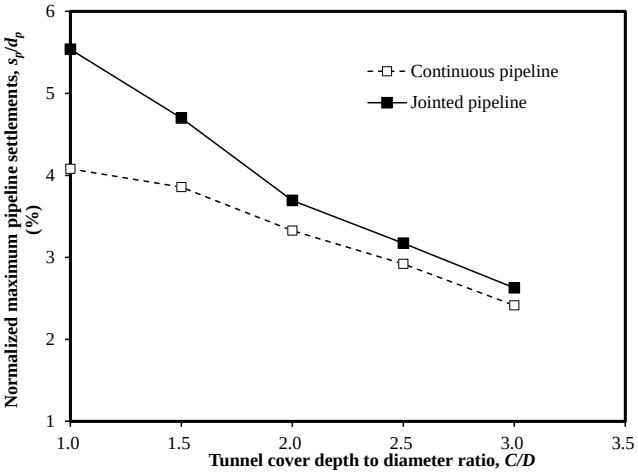

Fig. 6 Effects of tunnel burial depth on tunnel excavation-induced pipeline settlement

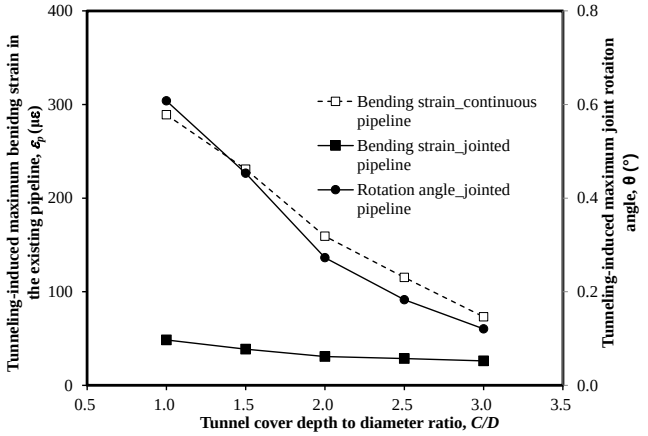

Fig. 7 Effects of tunnel cover depth to diameter ratio on tunneling-induced pipeline bending strain and joint rotation angle

pipelines, releasing bending constrains.

Although bending strains induced in the jointed pipelines are substantially reduced, tunneling-induced joint rotation in discontinuous pipelines are noticeable. For jointed pipelines with burial depths of 0.2C, 0.4C, 0.6C and 0.8C, tunneling-induced maximum joint rotation angles are 0.129°, 0.166°, 0.225° and 0.327°, respectively. Obviously, as pipeline burial depth is located closer to the new tunnel, tunneling-induced joint rotation angle increases at an increased rate. As reported by Molnar *et al*. (2003), the allowable joint rotation angle for serviceability state of existing pipeline is 0.275°. Note that tunneling-induced maximum joint rotation angle exceeds the allowable value when the burial depth of existing pipeline is 0.8 times of the tunnel cover depth. Obviously, the clear distance between the pipeline and tunnel has great effects on pipeline deformation. For this scenario, countermeasures may be adopted to alleviate tunneling induced adverse effects on existing pipelines.

In literature, jointed pipelines are simplified as continuous structures by applying a reduced flexural stiffness to consider the existences of joints along the pipeline. However, this method still assumes the pipeline as a continuous structure, and joint rotation angle cannot be obtained. Since tunneling-induced bending strain of jointed pipeline is relatively small, the serviceability and safety of jointed pipeline are controlled by joint rotation rather than bending moment. In order to evaluate the safety of existing pipelines due to tunnel excavation, pipeline joints should be directly simulated in the numerical analysis.

4.2 Effects of tunnel cover depth to diameter ratio on pipeline responses

Fig. 6 shows the effects of tunnel cover depth to diameter ratio on pipeline settlement. When tunnel cover depth to diameter ratios (*C/D*) are 1.0, 1.5, 2.0, 2.5 and 3.0, tunneling-induced maximum settlements in the continuous pipelines are 4.08%d_p, 3.86%d_p, 3.33%d_p, 2.92%d_p, and 2.41%d_p, respectively. Obviously, tunneling-induced maximum pipeline settlement is decreased as an increase in tunnel *C/D* ratio. By increasing tunnel *C/D* ratio from 1.0 to 3.0, tunneling-induced maximum settlements in the existing pipelines decrease by 38%. This is because much less stress relief is induced in the soil surrounding the existing pipelines as a new tunnel is constructed far away from the existing pipeline.

When the tunnel cover to diameter ratios (*C/D*) are 1.0, 1.5, 2.0, 2.5 and 3.0, tunneling-induced maximum settlements in the existing jointed pipelines are 5.54%d_p, 4.70%d_p, 3.69%d_p, 3.17%d_p, and 2.63%d_p, respectively. By increasing tunnel *C/D* ratio from 1.0 to 3.0, tunneling-induced maximum settlements in jointed pipelines are reduced by 53%. Because of joint rotation in discontinuous pipelines, tunneling-induced maximum settlements in the jointed pipelines are 8.8%-35.7% larger than that of continuous pipelines, as tunnel *C/D* ratio varies from 1.0 to 3.0. Due to the existence of joints, the overall flexural stiffness of jointed pipelines is smaller than of continuous pipelines, which has much less resistances to deform with soils surrounding the existing pipelines.

Fig. 7 compares bending strain and joint rotation of continuous and jointed pipelines. As expected, the maximum bending strains of pipelines are decreased as an increase in tunnel cover-to-diameter ratio (*C/D*). When the tunnel *C/D* ratios are 1.0, 1.5, 2.0, 2.5 and 3.0, tunneling-induced maximum bending strains in the continuous pipelines are 289, 231, 159, 115, and 73 με, respectively. By increasing the tunnel *C/D* ratio from 1.0 to 3.0, tunneling-induced maximum bending strain in the continuous pipeline is reduced by 74.7%. This is because a new tunnel constructed at a deep depth causing less stress changes in soil surrounding the existing pipeline.

Because of joint rotation, tunneling-induced maximum bending strains in the jointed pipelines are only 38.7, 30.7, 28.6, 26.0 $\mu\varepsilon$, respectively, for tunnel *C/D* ratios of 1.0, 1.5, 2.0, 2.5 and 3.0. Obviously, tunneling-induced maximum bending strains in the jointed pipelines are only 16.8%-35.6% of that of continuous pipelines. It should be noted that tunneling-induced joint rotation angles in the discontinuous pipelines are noticeably. As the tunnel *C/D* ratios are 1.0, 1.5, 2.0, 2.5 and 3.0, the induced maximum

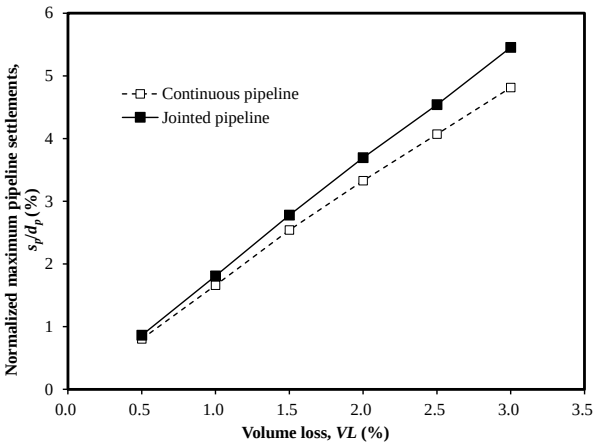

Fig. 8 Effects of tunnel volume loss on tunnel excavation-induced pipeline settlement

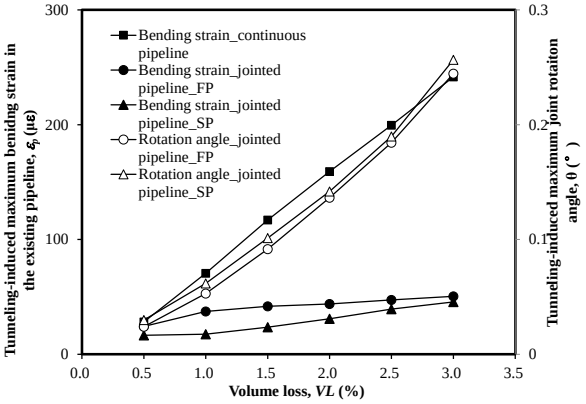

Fig. 9 Effects of tunnel volume loss on tunneling-induced maximum bending strain and joint rotation angle in existing pipelines

joint rotation angles are 0.608°, 0.453°, 0.273°, 0.183° and 0.121°, respectively. When the tunnel *C/D* ratio is less than 2.0, tunneling-induced joint rotation angle in the discontinuous pipelines exceeds the allowable value (0.275°) given by Molnar *et al*. (2003). Asa decrease in tunnel *C/D* ratio, tunneling-induced additional load exerted on pipeline is increased, i.e., causing much larger settlement and bending strain. As a result of joint rotation, tunneling-induced additional loads are mainly taken by joint rotation. Thus, tunneling-induced bending strains in the jointed pipelines have no obvious correlations with tunnel *C/D* ratios. Again, it is indicated that joints should be directly simulated in the analysis of tunnel-soil-pipeline interaction problem.

4.3 Effects of volume loss on pipeline responses

In reality, the volume loss due to shield tunneling commonly varies from 0.5% to 1.5% (Shi *et al*. 2016b). In order to obtain general results, a relatively large volume loss ranging from 0.5% to 3% is considered in this study. Fig. 8 shows the effects of volume loss on tunneling-induced maximum pipeline settlements. As expected, the maximum settlements of continuous and jointed pipelines due to tunnel excavation increase with volume loss. When the volume losses are 0.5%, 1.0%, 1.5%, 2.0%, 2.5%, and 3.0%, the maximum settlements of continuous pipelines are 0.80%d_p, 1.66%d_p, 2.54%d_p, 3.33%d_p, 4.07%d_p and 4.81%d_p, respectively. As an increase in the volume loss, tunneling-induced maximum pipeline settlements increases approximately linearly. By increasing the tunnel volume loss from 0.5% to 3.0%, tunneling-induced maximum pipeline settlements increases by 5 times. It is indicated that the volume loss has a great influence on the pipeline settlements. This is mainly because the greater the volume loss, the greater stress release caused by tunnel excavation.

Because of joint rotation, tunneling-induced maximum settlements in the jointed pipelines are 0.86%d_p, 1.81%d_p, 2.78%d_p, 3.69%d_p, 4.54%d_p and 5.45%d_p, respectively, for volume losses of 0.5%, 1.0%, 1.5%, 2.0%, 2.5% and 3.0%. As tunnel volume loss varies from 0.5% to 1.5%, the maximum settlements of jointed pipeline are 7.1%-13.3% larger than that of continuous pipeline. At a small volume loss, tunneling-induced ground settlement is small. Even though continuous pipeline can deform with surrounding soil movements. Thus, the differences in the maximum settlements of continuous and jointed pipelines at a small volume loss are negligible. As tunnel volume loss is increased, tunnel excavation induces excessive ground settlements, causing large resistances for pipeline deformed with surrounding soils. Moreover, the existence of joints decreases the flexural stiffness of discontinuous pipelines. Thus, the differences in the maximum settlements of continuous and jointed pipelines at a large volume loss are much more noticeable.

Fig. 9 compares tunneling-induced bending strain and joint rotation angles in the existing pipelines at different volume losses. When the volume losses are 0.5%, 1.0%, 1.5%, 2.0%, 2.5% and 3.0%, tunneling-induced maximum bending strains in the continuous pipeline are 28.3, 70.5, 117.0, 159.2, 199.6 and 241.7 με, respectively. Because of joint rotation in discontinuous pipelines, tunneling-induced maximum bending strains of jointed pipelines are decreased substantially. For jointed pipeline with flexible segments (i.e., FP), tunneling-induced maximum bending strains are 24.3, 37.3, 41.8, 43.9, 47.3 and 50.5 με, respectively. Moreover, tunneling-induced corresponding joint rotation angles are 0.024°, 0.053°, 0.092°, 0.136°, 0.184° and 0.245°, respectively. By increasing the volume loss from 0.5% to 3.0%, the maximum bending strains of continuous pipeline increases by 7.5 times. Moreover, the maximum bending strains of jointed pipeline only increases by 1.08 times, but its joint rotation angles increases by 9.20 times. Obviously, joint rotations induced in the discontinuous pipelines are much more vulnerable to tunnel volume loss. Thus, much more attention should be paid to tunneling-induced joint rotation rather than bending strain of jointed pipelines.

For the relatively stiff jointed pipeline (i.e., SP), tunneling-induced maximum bending strains are 16.6, 17.5, 23.6, 30.9, 39.4 and 45.6 με, respectively, for the tunnel volume losses of 0.5%, 1.0%, 1.5%, 2.0%, 2.5% and 3.0%. The corresponding joint rotation angles of jointed pipelines with stiff pipe segment (i.e., SP) are 0.030°, 0.062°, 0.101°,

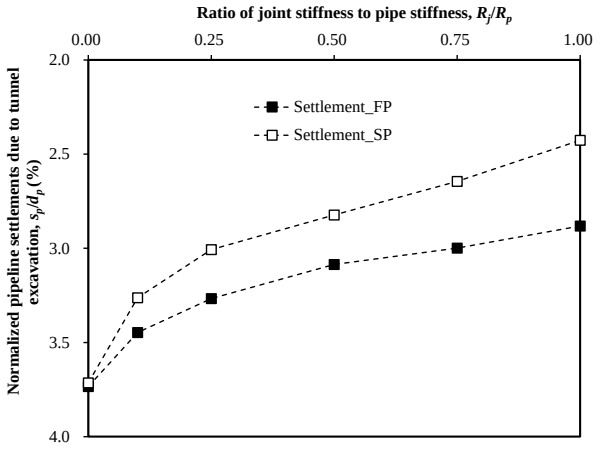

Fig. 10 Effects of joint stiffness on tunneling-induced maximum settlements in existing pipelines

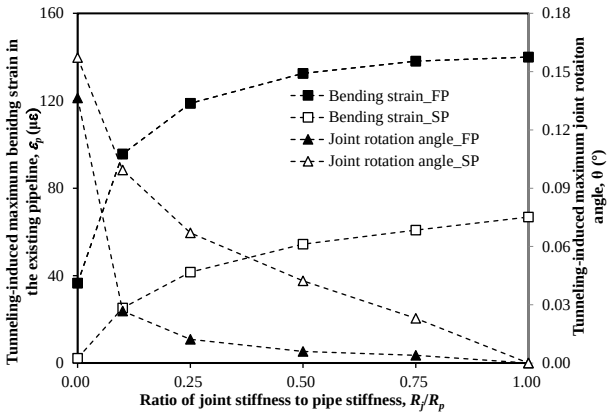

Fig. 11 Effects of joint stiffness on tunneling-induced maximum bending strain and joint rotation angle in existing pipelines

0.141°, 0.190° and 0.257°, respectively. As the flexural stiffness of pipe segment increases from 3.39×10^2 (i.e., FP) to 6.30×10^3 (i.e., SP), tunneling-induced bending strains of jointed pipelines are reduced by 9.6%-53.1%. Accordingly, much more additional loads induced by tunneling are taken by joint rotation. Consequently, joint rotation angles induced in the relatively stiff pipeline is 2.9%-24.1% larger than that of the relatively flexible pipeline.

4.4 Effects of joint stiffness on pipeline responses

Fig. 10 shows variations of tunneling-induced maximum pipeline settlements with joint stiffness. The joint stiffness R_j is normalized by the pipe segment stiffness R_p. The ratio R_j/R_p of 1 means that the pipeline is a continuous structure, otherwise it is a discontinuous structure. Moreover, he ratio R_j/R_p of 0 means that the joint is completely flexible.

When the ratios of joint stiffness to pipe segment stiffness are 0.00, 0.10, 0.25, 0.50, 0.75 and 1.00, tunneling-induced maximum settlements in the relatively flexible pipelines (i.e., FP) are 3.73%d_p, 3.45%d_p, 3.26%d_p, 3.08%d_p, 3.00%d_p and 2.88%d_p, respectively. For tunneling underneath jointed pipeline with relatively stiff pipe segments (i.e., SP), tunneling-induced maximum pipeline settlements are 3.71%d_p, 3.26%d_p, 3.00%d_p, 2.82%d_p, 2.64%d_p and 2.43%d_p, respectively, as joint stiffness ratios are 0.00, 0.10, 0.25, 0.50, 0.75 and 1.00. As joint stiffness ratio is increased, the overall flexural stiffness of the existing pipeline is increased. Consequently, tunneling-induced maximum settlements decreases dramatically as joint stiffness is increased. By increasing the joint stiffness ratio from 0.00 to 1.00, tunneling-induced maximum pipeline settlements are decreased by 22.8% to 34.7%.

Fig. 11 shows variations of joint rotation angle and bending strain of existing pipelines with joint stiffness ratio. By increasing the joint stiffness ratio, tunneling-induced joint rotation angle decreases dramatically, while bending strain due to tunnel excavation increases substantially instead. As an increase in the joint stiffness ratio, the dominated deformation mechanics of existing pipeline is shifted from joint rotation to bending strain. When the ratios of joint stiffness to pipe segment stiffness are 0.00, 0.10, 0.25, 0.50, 0.75 and 1.00, tunneling-induced maximum joint rotation angles in relatively flexible pipelines are 0.136°, 0.027°, 0.012°, 0.006°, 0.004° and 0.0°, respectively. Moreover, the maximum bending strains due to tunnel excavation are 36.6, 95.7, 118.8, 132.5, 138.2 and 140.0 με, respectively. As an increase in the flexural stiffness of pipe segment, bending deformation of pipe segment decreases, as expected. Thus, more and more additional loads due to tunnel excavation are taken by joint rotation.

When joint stiffness is very small, the joint can be considered as a hinge and cannot transfer any bending moment. Thus, the existence of joint cause a reduction in bending moment, but a large joint rotation angle. For tunneling underneath jointed pipeline with relatively stiff pipe segments (i.e., SP), the maximum bending strains decrease to 2.2, 25.2, 41.6, 54.4, 60.8 and 66.8 με, which are dramatically smaller than that of relatively flexible pipelines (i.e., SP). In contrast, tunneling-induced joint rotation angles in relatively stiff pipeline (i.e., SP) increases to 0.157°, 0.099°, 0.067°, 0.042°, 0.025° and 0.0°, which are significantly larger than that of flexible pipeline. Thus, much more attention should be paid to joint rotation of discontinuous pipeline with large flexural stiffness of pipe segment.

5. Conclusions

In this study, three-dimensional numerical analyses were conducted to investigate deformation characteristics of continuous and jointed pipelines due to underneath tunnel construction. Effects of pipeline burial depth, tunnel burial depth, volume loss, joint stiffness and pipeline stiffness on bending strain and joint rotation of existing pipelines were explored. Based on the computed results, the following conclusions can be drawn:

- By increasing pipeline burial depth ratio (i.e., c_p/C) from 0.2 to 0.8, tunneling-induced maximum settlements in continuous and jointed pipelines increase by 20.2% and 43.8%, respectively. Because of joint rotation in discontinuous pipelines, tunneling-induced maximum settlements in jointed pipelines are 10.1%-

31.8% larger than that of continuous pipelines, while the maximum bending strains of jointed pipelines are only 14.6%-26.7% of that induced in the continuous pipelines.

• As an increase in tunnel *C/D* ratio, tunneling-induced pipeline responses are reduced, as expected. For tunnel *C/D* ratio ranging from 1.0 to 3.0, tunneling-induced maximum settlements in jointed pipelines are 8.8%-35.7% larger than that of continuous pipelines, but the maximum bending strains of jointed pipelines are only 16.8%-35.6% of that of continuous pipelines. Tunneling-induced maximum joint rotation angle exceeds the allowable value when c_p/C is large than 0.8 or *C/D* ratio is less than 2.0.

• When the volume loss increases from 0.5% to 3.0%, tunneling-induced maximum settlements and bending strains in continuous pipelines increase by 5.0 and 7.5 times, respectively. However, the maximum bending strain of jointed pipeline only increases by 1.08 times, but its joint rotation angle increases by 9.20 times. Obviously, joint rotation induced in the discontinuous pipelines is much more vulnerable to tunnel volume loss.

• For tunneling underneath jointed pipelines, bending moment and joint rotation are induced simultaneously. When the flexural stiffness of pipe segment increases by 18.5 times, tunneling-induced bending strains in jointed pipelines are reduced by 9.6%-53.1%, while joint rotation angles induced in the relatively stiff pipeline increase by 2.9%-24.1%. This is because a stiff pipeline has large resistance to bend with surrounding soils, much more additional loads due to tunneling are taken by joint rotation.

• By increasing the joint stiffness ratio, tunneling-induced joint rotation angle decreases dramatically, while bending strain due to tunnel excavation increases substantially instead. The dominated deformation mechanism of existing pipeline is shifted from joint rotation to bending strain, as an increase in joint stiffness. When the joint stiffness ratio varies from 0.0 to 1.0, tunneling-induced maximum pipeline settlements decrease by 22.8%-34.7%. If a jointed pipeline is simplified as a continuous structure, tunneling-induced settlement is thus underestimated, but bending strain is grossly overestimated. Thus, joints should be directly simulated in the analysis of tunnel-soil-pipeline interaction.

Acknowledgments

This work is supported by the National Natural Science Foundation of China (51608170), Shenzhen Science and Technology Program (KCXFZ20211020163816023), and the Key Scientific Research Project of Zhejiang College of Security Technology (AF2021Z01).

References

Addenbrooke, T.I., Potts, D.M. and Puzrin, A.M. (1997), "The influence of pre-failure soil stiffness on the numerical analysis of tunnel construction", *Géotechnique*, **47**(3), 693-712. https://doi.org/10.1680/geot.1997.47.3.693.

Ardakani, A., Bayat, M. and Javanmard, M. (2014), "Numerical modeling of soil nail walls considering Mohr Coulomb, hardening soil and hardening soil with small-strain stiffness effect models", *Geomech. Eng.*, **6**(4), 391-401. https://doi.org/10.12989/gae.2014.6.4.391.

Attewell, P.B., Yeates, J. and Selby, A.R. (1986), *Soil Movements Induced by Tunneling and their Effects on Pipelines and Structures*, Blackie and Son Ltd., London.

Clayton, C.R.I. (2011), "Stiffness at small strain: Research and practice", *Géotechnique*, **61**(1), 5-37. https://doi.org/10.1680/geot.2011.61.1.5.

Fang, J.C., Kong, G.Q. and Yang, Q. (2022), "Group performance of energy piles under cyclic and variable thermal loading", *J. Geotech. Geoenviron. Eng.*, **148**(8), 04022060. https://doi.org/10.1061/(ASCE)GT.1943-5606.0002840.

Franza, A. and Marshall, A.M. (2019), "Empirical and semi-analytical methods for evaluating tunnelling-induced ground movements in sand", *Tunnel. Underg. Space Technol.*, **88**, 47-62. https://doi.org/10.1016/j.tust.2019.02.016.

Guan, X.M., Wang, X.C., Zhu, Z., Zhang, L. and Fu, H.X. (2020), "Ground vibration test and dynamic response of horseshoe-shaped pipeline during tunnel blasting excavation in pebbly sandy soil", *Geotech. Geolog. Eng.*, **38**(4), 3725-3736. https://doi.org/10.1007/s10706-020-01249-x.

Huang X., Huang, H.W. and Zhang, D.M. (2014), "Centrifuge modelling of deep excavation over existing tunnels", *Proc. ICE-Geotech. Eng.*, **167**(2), 3-18. https://doi.org/10.1680/geng.11.00045.

Huang, M.S., Zhou, X.C., Yu, J., Leung, C.F. and Tan, J.Q.W. (2019), "Estimating the effect of tunneling on existing jointed pipelines based on Winkler model", *Tunnel. Underg. Space Technol.*, **86**, 89-99. https://doi.org/10.1016/j.tust.2019.01.015.

Ieronymaki, E.S. and Whittle, A.J. (2017), "Pipeline response to ground deformations induced by tunneling", *Geotech. Spec. Publ.*, **277**, 566-575. https://doi.org/10.1061/9780784480441.059.

Klar, A., Marshall, A.M., Soga, K. and Mair, R.J. (2008), "Tunneling effects on jointed pipelines", *Can. Geotech. J.*, **45**(1), 131-139. https://doi.org/10.1139/T07-068.

Klar, A., Vorster, T.E.B., Soga, K. and Mair, R.J. (2005), "Soil-pipe-tunnel interaction: Comparison between Winkler and elastic continuum solutions", *Géotechniq.*, **55**(6), 461-466. https://doi.org/10.1680/geot.2005.55.6.461.

Lu, H., Shi, J.W., Ng, C.W.W. and Lv, Y.R. (2020), "Three-dimensional centrifuge modeling of the influence of side-by-side twin tunneling on a piled raft", *Tunnel. Underg. Space Technol.*, **103**, 103486. https://doi.org/10.1016/j.tust.2020.103486.

Ma, S.K., Liu, Y., Lv, X.L., Shao, Y. and Feng, Y. (2018), "Settlement and load transfer mechanism of pipeline due to twin stacked tunneling with different construction sequences", *KSCE J. Civil Eng.*, **22**(10), 3810-3817. https://doi.org/10.1007/s12205-018-0302-5.

Ma, S.K., Shao, Y., Liu, Y., Jiang, J. and Fan, X.L. (2017), "Responses of pipeline to side-by-side twin tunnelling at different depths: 3d centrifuge tests and numerical modelling", *Tunnel. Underg. Space Technol.*, **66**, 157-173. https://doi.org/10.1016/j.tust.2017.04.006.

Molnar, K.M., Finno, R.J. and Rossow, E.C. (2003), "Analysis of effects of deep braced excavations on adjacent buried utilities", Report for the U.S. Department of Transportation, No. A450, A464, Northwestern University, Illinois.

Ng, C.W.W., Lu, H. and Peng, S.Y. (2013), "Three-dimensional centrifuge modelling of twin tunnelling effects on an existing pile", *Tunnel. Underg. Space Technol.*, **35**(3), 189-199. https://doi.org/10.1016/j.tust.2012.07.008.

Rebello, N.E., Shivashankar, R. and Sastry, V.R. (2018), "Surface displacements due to tunneling in granular soil in presence and absence of geosynthetic layer under footings", *Geomech. Eng.*, **15**(2), 739-744. https://doi.org/10.12989/gae.2018.15.2.739.

Saiyar, M., Moore, I.D. and Take, W.A. (2015), "Kinematics of jointed pipes and design estimates of joint rotation under differential ground movements", *Can. Geotech. J.*, **52**(11), 1714-1724. https://doi.org/10.1139/cgj-2014-0347.

Shi, J.W., Chen, Y.H., Lu, H., Ma, S.K. and Ng, C.W.W. (2022a), "Centrifuge modeling of the influence of joint stiffness on pipeline response to underneath tunnel excavation", *Can. Geotech. J.*, https://doi.org/10.1139/cgj-2020-0360.

Shi, J.W., Wang, Y. and Ng, C.W.W. (2016a), "Numerical parametric study of tunneling-induced joint rotation angle in jointed pipelines", *Can. Geotech. J.*, **53**(12), 2058-2071. https://doi.org/10.1139/cgj-2015-0496.

Shi, J.W., Wang, Y. and Ng, C.W.W. (2016b), "Three-dimensional centrifuge modeling of ground and pipeline response to tunnel excavation", *J. Geotech. Geoenviron. Eng.*, **142**(11), 04016054. https://doi.org/10.1061/(ASCE)GT.1943-5606.0001529.

Shi, J.W., Wei, J.Q., Ng, C.W.W., Lu, H. Ma, S.K., Shi, C. and Li, P. (2022b), "Effects of construction sequence of double basement excavations on an existing floating pile", *Tunnel. Underg. Space Technol.*, **119**, 104230. https://doi.org/10.1016/j.tust.2021.104230.

Shi, J.W., Zhang, X. Chen, L. and Chen, L. (2017), "Numerical investigation of pipeline responses to tunneling-induced ground settlements in clay", *Soil Mech. Found. Eng.*, **54**(5), 303-309. https://doi.org/10.1007/s11204-017-9473-1.

Shirlaw, J.N., Ong, J.C.W., Rosser, H.B., Tan, C.G., Osborne, N.H. and Heslop, P.E. (2003), "Local settlements and sinkholes due to EPB tunnelling", *Geotech. Eng.*, **156**(4), 193-211. https://doi.org/10.1680/geng.2003.156.4.193.

Soomro, M.A., Kumara, M., Xiong, H., Mangnejo, D. and Mangia, N. (2020), "Investigation of effects of different construction sequences on settlement and load transfer mechanism of single pile due to twin stacked tunnelling", *Tunnel. Underg. Space Technol.*, **96**, 103171. https://doi.org/10.1016/j.tust.2019.103171.

Tan, Y. and Li, M. (2011), "Measured performance of a 26 m deep top-down excavation in downtown Shanghai", *Can. Geotech. J.*, **48**(5), 704-719. https://doi.org/10.1139/T10-100.

Vorster, T.E.B., Klar, A., Soga, K. and Mair, R.J. (2005), "Estimating the effects of tunneling on existing pipelines", *J. Geotech. Geoenviron. Eng.*, **131**(11), 1399-1410. https://doi.org/10.1061/(ASCE)1090-0241(2005)131:11(1399).

Wang, Y., Kong, L.W., Wang, Y.L. and Li, X.W. (2018), "Safety analysis for the underground pipelines close to a subway foundation pit under small soil strains", *Geotech. Spec. Publ.*, **304**, 527-541. https://doi.org/10.1061/9780784482049.051.

Wham, B.P., Argyrou, C. and O'rourke, T.D. (2016), "Jointed pipeline response to tunneling-induced ground deformation", *Can. Geotech. J.*, **53**(11), 1794-1806. https://doi.org/10.1139/cgj-2016-0054.

Yamashita, S., Jamiolkowski, M. and Lo Presti, D.C.F. (2000), "Stiffness nonlinearity of three sands", *J. Geotech. Geoenviron. Eng.*, **126**(10), 929-938. https://doi.org/10.1061/(ASCE)1090-0241(2000)126:10(929).

Yu, J., Zhang, C.R. and Huang, M.S. (2013), "Soil-pipe interaction due to tunnelling: Assessment of Winkler modulus for underground pipelines", *Comput. Geotech.*, **50**, 17-28. https://doi.org/10.1016/j.compgeo.2012.12.005.

Zhang, K.Y., Torres, J. and Zang, Z.J. (2019), "Numerical analysis of pipelines settlement induced by tunneling", *Adv. Civil Eng.*, **55**, 1-10. https://doi.org/10.1155/2019/4761904.

Zhang, Z.G., Zhang, M.X., Zhao, Q.H., Fang, L., Ding, Z. and Shi, M.Z. (2021), "Interaction analyses between exiting pipeline and quasi-rectangular tunneling in clays", *KSCE J. Civil Eng.*, **25**(1), 326-344. https://doi.org/10.1007/s12205-020-2366-2.

Zhang, Z.G., Zhao, Q.H. and Zhang, M.X. (2016), "Deformation analyses during subway shield excavation considering stiffness influences of underground structures", *Geomech. Eng.*, **11**(1), 117-139. https://doi.org/10.12989/gae.2016.11.1.117.

Zhu, J.L. and Zhu, D.Y. (2020), "Deformation of pipelines induced by the construction of underlying twin-tunnel", *Tehnicki Vjesnik*, **27**(4), 1311-1315. https://doi.org/10.17559/TV-20191118080659.

GC